Physica E 47 (2013) 316–323

Contents lists available at SciVerse ScienceDirect

Physica E

journal homepage: www.elsevier.com/locate/physe

Torsional instability of carbon nano-peapods based on the nonlocal elastic shell theory

M. Asghari *, J. Rafati, R. Naghdabadi

School of Mechanical Engineering, Sharif University of Technology, Azadi, Tehran, Iran

HIGHLIGHTS

- Nonlocal elastic shell model can predict the torsional instability of nanopeapods.
- Nonlocal results are somehow in good agreement with MD simulations.
- Instability resistance of (10,10) CNT is increased by encapsulating C_{60} fullerenes.

GRAPHICAL ABSTRACT

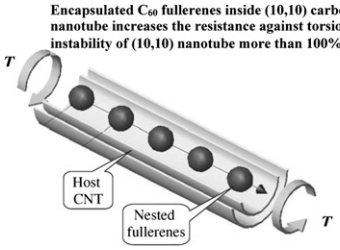

ARTICLE INFO

Article history:
Received 28 February 2012
Received in revised form
16 June 2012
Accepted 22 June 2012
Available online 28 June 2012

ABSTRACT

In this paper a shell formulation is proposed for analyzing the torsional instability of carbon nano-peapods (CNPs), i.e., the hybrid structures composed of C_{60} fullerenes encapsulated inside carbon nanotubes (CNTs), based on the nonlocal elasticity theory. The nonlocal elasticity theory, as a well-known non-classical continuum theory, is capable to capture small scale effects which appear due to the discontinuities in nano-structures. Based on the derived formulation, the critical torsional moments for a pristine (10,10) CNT and C_{60}@(10,10) CNP are investigated as case studies. The results for the (10,10) CNT are compared with those of the available molecular dynamics simulations in the literature, and accordingly the appropriate value of the small scale coefficient appearing in the constitutive equations of the nonlocal theory is estimated for CNTs. Then, the critical torsional moment for the C_{60}@(10,10) CNP is predicted. It is observed that the presence of the encapsulated C_{60} fullerenes inside the (10,10) CNT causes an increase in the torsional instability resistance of the CNT more than 100%.

1. Introduction

Carbon nanotubes (CNTs) are found out capable to absorb and encapsulate some molecules and nanostructures [1–8]. For example, it has been observed that C_{60} fullerenes can be encapsulated inside CNT [8,9]; the resulted hybrid nano-structure is called the carbon nano-peapod (CNP) or C_{60}-peapod [7–9]. The encapsulating process is spontaneous for a single-walled carbon nanotube (SWCNT) with diameter in range of 1.3–1.4 nm [8,9], e.g., (10,10) CNT [10]. This range of diameter for host CNT makes a proper space for the nested C_{60} fullerenes to maintain a preferred graphitic van der Waals (vdW) separation (i.e., ~0.3 nm) from the CNT's internal wall [8–10]. The encapsulated C_{60} fullerenes may change the physical, electrical and mechanical characteristics of CNT [7,10]. The characteristics of the new hybrid nano-structure (i.e., CNP) have been found interesting, unique and different with respect to the properties of a single unfilled CNT [7,10]. This fact has motivated researchers to find possible applications of these new hybrid nano-structures [7]. As a result, investigation of structural stability and mechanical behaviors of CNPs have attracted some researchers [11–18]. Here, some studies on the instability of C_{60}-peapods based on the molecular

* Corresponding author. Tel.: +98 21 66165523; fax: +98 21 66000021.
E-mail address: asghari@sharif.edu (M. Asghari).

1386-9477/$ - see front matter © 2012 Elsevier B.V. All rights reserved.
http://dx.doi.org/10.1016/j.physe.2012.06.016

dynamics (MD) simulations are reviewed. The effect of filling a (10,10) CNT with C_{60} fullerenes on instability of unfilled (10,10) CNT under axial compressive load [12,13] and bending moment [14] have been investigated using MD simulations. In addition, the effect of the presence of the C_{60} fullerenes on the torsional stability of (10,10) CNT have been studied by Jeong et al. [15] and Wang [16], based on the MD simulations. All the results state that the resistance of the hybrid structure C_{60}@(10,10) CNP against instability is more than the unfilled (10,10) CNT [12–16].

Although, MD simulations can potentially give accurate results in the simulation of nano-structures, but they are computationally expensive for systems with large sizes. [19]. Therefore, some researchers have moved towards applying models based on the continuum mechanics for analyzing and studying the nanostructures to arrive at the results with much less computational costs. The classical shell theory, as a continuum based theory, has widely been employed in the literature to model CNTs to predict their mechanical behaviors. For instance, the buckling stability of CNTs under axial loading [20,21], uniform external pressure [22], bending [23] and torsional moments [24] has been investigated based on the classical shell theories. Also, stability investigation of C_{60}-peapods under hydrostatic pressure [17] and also torsional moment [18] has been presented in the literature. In nanostructures, the discontinuity between material atoms is significant when compared with the overall dimensions. This fact makes the implementation of classical continuum theory doubtful for analyzing the nano-structures [25–30]. In other words, the classical continuum theory which neglects the small scale effects and natural discontinuity of atomic range structures should essentially be replaced with appropriate non-classical ones which consider the small scale effects and produce reliable results [25–31]. The "nonlocal continuum theory", introduced by Eringen [32,33], is one of the non-classic theories in which the small scale effects are considered in writing the constitutive equations. Recently, much attention has been directed to modeling of nano-structures, specially CNTs, by using the nonlocal continuum-based theories, in studying the mechanical behavior of CNTs [25,26,29–31,34]. The nonlocal shell modeling of CNTs is a powerful approach for getting more reliable results in the continuum based methods. For example, the stability of CNTs and also nano-peapods under external pressure [35], axial loading [36], and torsional loading [37] has been investigated by the researchers using the nonlocal elastic shell models. In addition, the thermal buckling [31], vibration behavior [38] and wave propagation phenomenon [27] of CNTs have been studied employing the nonlocal elastic shell model. In this paper, the torsional stability of multi-walled carbon nano-peapods (MWCNP) is investigated using the nonlocal elastic shell model. The results of case studies are compared with available MD simulation reports.

2. The vdW interactions in C_{60}-peapods

2.1. VdW interaction between nested fullerenes and host carbon nanotube

The inter-atomic non-bonded vdW interactions between the encapsulated C_{60} fullerenes and the host carbon nanotube (see Fig. 1) can be described using a form of Lenard-Jones (LJ) potential functions as [11]

$$\phi_{ab} = \frac{A}{d_{CC}^6}\left[\frac{1}{2}y_0^6\left(\frac{d_{CC}}{r_{ab}}\right)^{12} - \left(\frac{d_{CC}}{r_{ab}}\right)^{6}\right], \tag{1}$$

where r_{ab} stands for the distance between atom a of the CNT and atom b of C_{60} fullerenes, and $A=24.3\times10^{-79}$ J m^6, $d_{CC}=1.42$ Å, $y_0=2.7$. Using the LJ potential function in Eq. (1), the inter-atomic

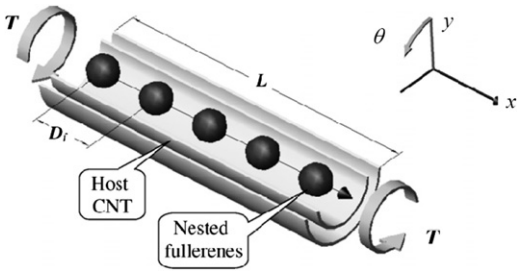

Fig. 1. The schematic view of a C_{60}-peapod subjected to a torsional moment.

vdW force between atom a of CNT and atom b of C_{60} can be obtained as:

$$F_{ab} = -\frac{d\varphi_{ab}}{dr_{ab}} = \frac{6A}{{d_{CC}}^5}\left[y_0^6\left(\frac{d_{CC}}{r_{ab}}\right)^{13} - \left(\frac{d_{CC}}{r_{ab}}\right)^{7}\right]. \tag{2}$$

The total vdW force exerted on atom a of the host CNT is determined by summing of all radial component of F_{ab} on all atoms b of the encapsulated C_{60} fullerenes in effective cut-off range of LJ potential; so one can write:

$$F_{\mathrm{vdW},a} = \sum_b (F_{ab})_r, \tag{3}$$

where, $F_{\mathrm{vdW},a}$ denotes the vdW radial force on atom a of CNT exerted by the C_{60} molecules and r denotes the radial coordinate of CNT.

Each atom of carbon occupies an equivalent area of $9d_{CC}/4\sqrt{3}$ in hexagonal lattice of CNT [20]; hence, the vdW radial pressure on the CNT wall in the position of atom a of the CNT can be obtained as:

$$p_{\mathrm{vdW},a} = F_{\mathrm{vdW},a}\left(9d_{CC}/4\sqrt{3}\right)^{-1}, \tag{4}$$

where $d_{CC}=1.42$ Å denotes the carbon–carbon covalent bond length in the graphitic lattice of CNT. Because of the repeated arrangement of C_{60} fullerenes inside the CNT, it is justifiable to assume the distribution of the pressure $p_{\mathrm{vdW}-C_{60}}$ exerted by C_{60} on CNT wall as an harmonic one [18]:

$$p_{\mathrm{vdW}-C_{60}}(x) = a_0 + \sum_q \left[a_n\cos\left(\frac{2q\pi x}{D_f}\right) + b_n\sin\left(\frac{2q\pi x}{D_f}\right)\right], \tag{5}$$

where a_n and b_n stand for the Fourier series constants. Also, D_f is the lattice equilibrium distance between the encapsulated C_{60} fullerenes.

2.2. The vdW interaction between CNT layers

The vdW interactions exerted on the i-th layer of nanotube from the j-th layer can be modeled as an equivalent pressure distribution p_{ij} in the following linear form [31,36]

$$p_{ij} = c(w_i - w_j), \tag{6}$$

where w_i denotes the radial displacement of the i-th layer of the multi-walled carbon nanotube (MWCNT), and constant c is the vdW interaction coefficient. The initial vdW pressure, before deflection of the layers, has been neglected in writing Eq. (6), as it is usual in the literature [23,24,31,37]. In view of the equilibrium equation of layers in the radial direction, one can conclude [31,37]

$$p_{ij}R_i = -p_{ji}R_j, \tag{7}$$

where R_i denotes the radius of the i-th layer of MWCNT.

2.3. The total vdW pressure on nanotube layers

Since, the vdW inter-atomic interaction is relatively weak; the effect of the non-adjacent layers can be neglected in determining the total radial pressure exerted on each layer of the nanotube. Similarly, only the interaction between the nested C_{60} fullerene atoms and the innermost layer of MWCNT is considerable. By these assumptions and substituting Eq. (6) into (7), the total pressure on each layer of MWCNT with k co-centric layers can be written as [18,31,36,37]

$$\begin{aligned} &p_1 = p_{12} = c(w_2 - w_1) + p_{vdW-C_{60}},\\ &p_i = p_{i(i-1)} + p_{i(i+1)} = c\left[w_{i+1} - w_i - (R_{i-1}/R_i)(w_i - w_{i-1})\right];\\ &\quad i = 2, \ldots, k-1,\\ &p_k = p_{k(k-1)} = c(R_{k-1}/R_n)(w_{k-1} - w_k). \end{aligned} \tag{8}$$

The numbering order of layers is from inside to outside, i.e., the innermost layer is assigned by number 1 and the outermost by k, respectively. It is noted that a repulsive interaction between objects is equivalent to a positive value for the pressure, and an attractive one is equivalent to a negative value.

Since the main objective of the manuscript is the rigorous presentation of a shell formulation for torsional stability of nanopeapods based on the nonlocal theory, a simple and phenomenological model for the van der Waals interactions has been considered as presented in Eq. (8). More accurate models for these interactions are also available in the literature (e.g., [39]).

3. Nonlocal shell model

In contrast to the classical theory, Eringen [32] proposed the idea of considering the effect of the state of strain at neighboring points of a considered point, say the local point, on the local stress state. The neighboring points are called the nonlocal ones. Based on this idea, he presented the nonlocal elasticity theory. This theory is capable to consider small scale effects. According to an integral form of the constitutive equation in the nonlocal theory, the stress tensor at a local point $\boldsymbol{x}$ is written as [19,33]:

$$\sigma(x) = \iiint_{\Omega} \psi(|x' - x|, \tau) C : \varepsilon(x') dV(x'), \tag{9}$$

where $\psi(|\boldsymbol{x}' - \boldsymbol{x}|, \tau)$is the nonlocal modulus function [19], $|\boldsymbol{x}' - \boldsymbol{x}|$ is the distance of $\boldsymbol{x}$ and a considered nonlocal point $\boldsymbol{x}'$. Also, $\boldsymbol{C}$ is the elasticity tensor which is mathematically a fourth-order tensor. Moreover, parameter τ is equal to $e_0 a/l$, in which a is the internal characteristic length, l is the external characteristic length, and e_0 is a material parameter determined for a nanostructure based on experimental results and nonlocal theory based simulations [19,31,33,36]. The differential form of constitutive equation in the nonlocal theory also is available which is written as follows [31,33]

$$\left(1 - \eta^2 \nabla^2\right) \sigma = C : \varepsilon. \tag{10}$$

Parameter η is called the small scale coefficient for the nonlocal elasticity. This parameter is calculated from the following relation

$$\eta = \tau l = e_0 a. \tag{11}$$

The component form of Eq. (10) is [19,27,31,36]:

$$\left(1 - \eta^2 \nabla^2\right) \sigma_{ij} = C_{ijkl} \varepsilon_{kl}. \tag{12}$$

The small scale parameter η, appearing in the constitutive Eq. (10), is indeed a nonclassical material property, beside the classical material properties (i.e., the Young's modulus and the Poisson's ratio) included in tensor $\boldsymbol{C}$. This small scale parameter for any specific material should be determined by performing appropriate experiments on that material. Recalling the mathematical interpretation of the Laplacian of a variable, e.g., $\nabla^2 \sigma_{ij}$, as a representation of the intensity of the mean difference of the value of σ_{ij} at a material point and its neighborhood points, and in view of the nonlocal constitutive Eq. (10), it is concluded that the value of strain components ε_{kl} at a material point depends both on its stress state components and the stress state of its neighborhoods. While in the classical theory with $\eta = e_0 a = 0$, the state of strain at a material point is only dependent on its own stress state. More is $\eta = e_0 a$, the effect of the stresses at neighborhoods is greater on the stress state of a considered material point. For in depth discussion on parameter η, study of [34] is suggested.

Now, we consider a tubular cylindrical shell with length L, mean radius R and thickness h. Let (x,θ,r) be the axial, circumferential and radial coordinates of the tube, respectively. The displacement field of the shell is described by (u_1,u_2,u_3). Based on the Donnell's assumptions for thin shells, the displacement field can be written as [42]:

$$\begin{aligned} u_1(x,\theta,r) &= u(x,\theta) - r' w_{,x}\\ u_2(x,\theta,r) &= v(x,\theta) - r' \frac{w_{,\theta}}{R}\\ u_3(x,\theta,r) &= w(x,\theta) \end{aligned} \tag{13}$$

where (u,v,w) denotes displacement components of the mid-surface, and $r' = r - R$ is the radial distance from the mid-surface. Also, a comma as an index of the variables denotes the differentiation with respect to the following variable. For thin shells, the mid-surface displacement components can be assumed independent of radial coordinate; also, the radial normal stress σ_r may be neglected with respect to σ_x and σ_θ for thin shells. According to the displacement field of Eq. (13), the components of the strain tensor $\boldsymbol{\varepsilon}$ can be written as [31,37]:

$$\begin{aligned} \varepsilon_x &= \tfrac{\partial u_1}{\partial x} = u_{,x} - r' w_{,xx}\\ \varepsilon_\theta &= \tfrac{1}{R}\tfrac{\partial u_2}{\partial \theta} + \tfrac{w}{R} = \tfrac{v_{,\theta}}{R} + \tfrac{w}{R} - r' \tfrac{w_{,\theta\theta}}{R^2}\\ \gamma_{x\theta} &= \tfrac{1}{R}\tfrac{\partial u_1}{\partial \theta} + \tfrac{\partial u_2}{\partial x} = \tfrac{u_{,\theta}}{R} + v_{,x} - 2r' \tfrac{w_{,x\theta}}{R}. \end{aligned} \tag{14}$$

By substituting the strain components from Eq. (14) into the constitutive equation of the nonlocal elasticity Eq. (12), the following expressions for the components of the stress tensor can be obtained as [19,29,31]:

$$\left(1 - \eta^2 \nabla^2\right) \begin{Bmatrix} \sigma_x\\ \sigma_\theta\\ \tau_{x\theta} \end{Bmatrix} = \frac{E}{1 - \nu^2} \begin{Bmatrix} \varepsilon_x + \nu \varepsilon_\theta\\ \varepsilon_\theta + \nu \varepsilon_x\\ (1-\nu)\gamma_{x\theta}/2 \end{Bmatrix} \tag{15}$$

where E and ν denote the elastic modulus and the Poisson's ratio of tube, and ∇^2 represents the Laplacian operator, which is given by:

$$\nabla^2 = \frac{\partial^2}{\partial x^2} + \frac{1}{R^2}\frac{\partial^2}{\partial \theta^2}. \tag{16}$$

The resultant axial, circumferential and shearing forces per unit circumferential length, respectively, parameters $N_x, N_\theta, N_{x\theta}$, can be written as [31]:

$$\begin{Bmatrix} N_x\\ N_\theta\\ N_{x\theta} \end{Bmatrix} = \int_{-h/2}^{h/2} \begin{Bmatrix} \sigma_x\\ \sigma_\theta\\ \sigma_{x\theta} \end{Bmatrix} dr', \tag{17}$$

By applying operator $(1 - \eta^2 \nabla^2)$ to both sides of Eq. (17), then substituting Eq. (15) into the result, one can arrive at:

$$\left(1 - \eta^2 \nabla^2\right) \begin{Bmatrix} N_x\\ N_\theta\\ N_{x\theta} \end{Bmatrix} = K \begin{Bmatrix} u_{,x} + \nu\left(v_{,\theta}/R + w/R\right)\\ v_{,\theta}/R + w/R + \nu u_{,x}\\ (1-\nu)\left(u_{,\theta}/R + v_{,x}\right)/2 \end{Bmatrix}. \tag{18}$$

where $K=Eh/(1-\nu^2)$ denotes the effective axial stiffness. Similarly, the resultant moments per unit circumferential length $(M_x,M_\theta,M_{x\theta})$ due to corresponding stress components $(\sigma_x,\sigma_\theta,\sigma_{x\theta})$ can be obtained as [31]:

$$\begin{Bmatrix} M_x \\ M_\theta \\ M_{x\theta} \end{Bmatrix} = \int_{-h/2}^{h/2} \begin{Bmatrix} \sigma_x \\ \sigma_\theta \\ \sigma_{x\theta} \end{Bmatrix} r' dr'. \tag{19}$$

Application of operator $(1-\eta^2\nabla^2)$ to both sides of Eq. (19), then substitution of Eq. (15) into the result, yields the following equations:

$$\left(1-\eta^2\nabla^2\right)\begin{Bmatrix} M_x \\ M_\theta \\ M_{x\theta} \end{Bmatrix} = -D\begin{Bmatrix} w_{,xx}+\nu w_{,\theta\theta}/R \\ w_{,\theta\theta}/R^2+\nu w_{,xx} \\ (1-\nu)w_{,x\theta}/R \end{Bmatrix}, \tag{20}$$

where $D=Eh^3/12(1-\nu^2)$ is the effective bending stiffness [31]. The equations of equilibrium of shell elements in terms of the resultant forces are [40]:

$$N_{x,x}+\frac{1}{R}N_{\theta x,y}=0, \tag{21}$$

$$N_{x\theta,x}+\frac{1}{R}N_{\theta,\theta}=0, \tag{22}$$

$$Q_{xr,x}+\frac{1}{R}Q_{\theta r,\theta}+\frac{\partial}{\partial x}\left(N_x\frac{\partial w}{\partial x}\right)+\frac{1}{R}\frac{\partial}{\partial x}\left(N_{x\theta}\frac{\partial w}{\partial \theta}\right) + \frac{1}{R}\frac{\partial}{\partial \theta}\left(N_{\theta x}\frac{\partial w}{\partial x}\right)+\frac{1}{R}\frac{\partial}{\partial \theta}\left(N_\theta\frac{\partial w}{\partial \theta}\right)-\frac{N_\theta}{R}-p=0, \tag{23}$$

where Q_{xr} and $Q_{\theta r}$ denote the shearing resultant forces in the radial direction, and p stands for the net pressure distribution on the surface of the shell. Also, the equations governing the rotational equilibrium of shell elements are written as [40]:

$$Q_{xr}=M_{x,x}+\frac{1}{R}M_{\theta x,\theta}, \tag{24}$$

$$Q_{\theta r}=M_{x\theta,x}+\frac{1}{R}M_{\theta,\theta}. \tag{25}$$

By substituting Eqs. (24) and (25) into Eq. (23), one can arrive at:

$$M_{x,xx}+2\frac{1}{R}M_{x\theta,x\theta}+\frac{1}{R^2}M_{\theta,\theta\theta}+\Im[w]-\frac{N_\theta}{R}-p=0, \tag{26}$$

with $\Im$ as a differential operator defined as follows [31,37]:

$$\Im=N_x\frac{\partial^2}{\partial x^2}+2N_{x\theta}\frac{1}{R}\frac{\partial^2}{\partial x\partial\theta}+N_\theta\frac{1}{R^2}\frac{\partial^2}{\partial\theta^2}. \tag{27}$$

Now, by applying operator $(1-\eta^2\nabla^2)$ to the equilibrium eqs. (21), (22) and (26), then substituting the resultants from Eqs. (18) and (20), we get

$$K\left[u_{,xx}+\nu\frac{v_{,x\theta}}{R}+\nu\frac{w_{,x}}{R}+\frac{(1-\nu)}{2}\left(u_{,\theta\theta}+\frac{v_{,x\theta}}{R}\right)\right]=0, \tag{28}$$

$$K\left[\frac{(1-\nu)}{2}\left(\frac{1}{R}u_{,x\theta}+v_{,xx}\right)+v_{,\theta\theta}+\frac{w_{,\theta\theta}}{R^2}+\nu\frac{1}{R}u_{,x\theta}\right]=0, \tag{29}$$

$$-D\left[w_{,xxxx}+\nu\frac{1}{R^2}w_{,xx\theta\theta}+\frac{1}{R^4}w_{,\theta\theta\theta\theta}+\nu\frac{1}{R^2}w_{,xx\theta\theta}+2(1-\nu)\frac{1}{R^2}w_{,xx\theta\theta}\right] + \left(1-\eta^2\nabla^2\right)\Im[w]-\frac{K}{R}\left(u_{,x}+\nu\frac{1}{R}v_{,\theta}+\nu\frac{w}{R}\right)-\left(1-\eta^2\nabla^2\right)p=0. \tag{30}$$

By eliminating u and v, the axial and circumferential components of the displacement vector, from Eqs. (28)–(30), the nonlocal equilibrium equation of a tubular Donnell's shell is obtained as [31,37]:

$$D\nabla^8 w+\frac{Eh}{R^2}\frac{\partial^4 w}{\partial x^4}-(1-\eta^2\nabla^2)\nabla^4\Im[w]-(1-\eta^2\nabla^2)\nabla^4 p=0. \tag{31}$$

4. Torsional buckling of carbon nano-peapods

Consider an MWCNP composed of an MWCNT with k layer of co-centric cylindrical tubes encapsulating an ordered arrangement of C_{60} fullerenes with lattice distance of D_f (Fig. 1). The total applied torque to the C_{60}@MWCNT peapod can be simply written as:

$$T=\sum_{j=1}^{k}T_j, \tag{32}$$

where T_j is the portion of the applied torsional moment on the j-th layer of MWCNT. The shearing resultant on each layer of MWCNT is proportional to the radius of that layer [37]. It means that,

$$\frac{N_{x\theta1}}{R_1}=\frac{N_{x\theta2}}{R_2}=\cdots=\frac{N_{x\theta j}}{R_j}=\cdots=\frac{N_{x\theta k}}{R_k}, \tag{33}$$

where, $N_{x\theta j}=T_j/2\pi R_j^2$ denotes the shearing resultant on the j-th layer. Substitution of Eq. (33) into (32) results in:

$$N_{x\theta j}=\frac{TR_j}{2\pi\sum_{m=1}^{k}R_m^3}. \tag{34}$$

In the case of applying a single torsional moment as the loading, the axial normal stresses in each layer of MWCNT vanish. Also, the circumferential normal stresses appear only because the possible presence of vdW pressure exerted on the layers. Accordingly, we have

$$N_{xi}=0,\quad N_{\theta i}=R_i p_i^0(x), \tag{35}$$

where $p_i^0(x)$ denotes the vdW pressure on the i-th layer of the MWCNT exerted by the nested C_{60} fullerenes. As stated before, the vdW pressure distribution exerted by the nested C_{60} fullerenes is only effective on the innermost nanotube, therefore $p_i^0(x)$ can be written as:

$$p_1^0(x)=p_{\mathrm{vdW},C_{60}}(x),\quad p_i^0(x)=0;\quad i=2,3,\ldots,k. \tag{36}$$

Substitution of Eq. (35) into (27) yields in the following result for operator $\Im$ in the j-th layer:

$$\Im_j=2N_{x\theta j}\frac{1}{R_j}\frac{\partial^2}{\partial x\partial\theta}+R_j p_j^0\frac{1}{R_j^2}\frac{\partial^2}{\partial\theta^2}, \tag{37}$$

Now, by substituting operator $\Im_j$ from Eq. (37) and also the pressure distribution from Eq. (8) into (31), the equilibrium equation for nanotube layers in the CNP is obtained as

$$D\nabla^8 w_1+\frac{Eh}{R_1^2}\frac{\partial^4 w_1}{\partial x^4}-\left(1-\eta^2\nabla^2\right)\nabla^4 \left\{2N_{x\theta1}\frac{1}{R_1}\frac{\partial^2}{\partial x\partial\theta}+R_1 p_{\mathrm{vdW},C60}(x)\frac{1}{R_1^2}\frac{\partial^2}{\partial\theta^2}\right\}w_1 - \left(1-\eta^2\nabla^2\right)\nabla^4\left[c(w_2-w_1)+p_{\mathrm{vdW},C_{60}}(x)\right]=0, \tag{38}$$

$$D\nabla^8 w_i+\frac{Eh}{R_i^2}\frac{\partial^4 w_i}{\partial x^4}-\left(1-\eta^2\nabla^2\right)\nabla^4\left\{2\frac{R_i}{R_1}\frac{1}{R_i}N_{x\theta1}\frac{\partial^2}{\partial x\partial\theta}\right\}w_i - \left(1-\eta^2\nabla^2\right)\nabla^4 c\left[w_{i+1}-w_i-(R_{i-1}/R_i)(w_i-w_{i-1})\right]=0; \quad i=2,\ldots,k-1, \tag{39}$$

$$D\nabla^8 w_k+\frac{Eh}{R_k^2}\frac{\partial^4 w_k}{\partial x^4}-\left(1-\eta^2\nabla^2\right)\nabla^4\left\{2\frac{R_k}{R_1}\frac{1}{R_k}N_{x\theta 1}\frac{\partial^2}{\partial x\partial\theta}\right\}w_k$$
$$-\left(1-\eta^2\nabla^2\right)\nabla^4 c\left[(R_{k-1}/R_k)(w_{k-1}-w_k)\right]=0. \quad (40)$$

Satisfaction of Eqs. (38)–(40) is necessary for the equilibrium of a CNP under a torsional moment in infinitesimal deformations with respect to the initial unloaded configuration. But, this does not suffice for the stability of the CNP. Let functions w_j denote the deflections of the corresponding infinitesimal deformation. For finding the critical value of the loading which corresponds to the start of the instability, here the critical torsional moment T_{cr}, we can consider the perturbation functions $\tilde{w}_j$ and expect that equilibrium Eqs. (38)–(40) to be again satisfied by replacing w_j with $\tilde{w}_j+\tilde{w}_j$. A complete discussion about this fact has been provided in [35]. Now, subtraction of the new equilibrium equations from the old ones results in:

$$D\nabla^8\tilde{w}_1+\frac{Eh}{R_1^2}\frac{\partial^4\tilde{w}_1}{\partial x^4}-\left(1-\eta^2\nabla^2\right)\nabla^4$$
$$\left\{2N_{x\theta 1}\frac{1}{R_1}\frac{\partial^2}{\partial x\partial\theta}+R_1 p_{\mathrm{vdW},C_{60}}(x)\frac{1}{R_1^2}\frac{\partial^2}{\partial\theta^2}\right\}\tilde{w}_1$$
$$-\left(1-\eta^2\nabla^2\right)\nabla^4[c(\tilde{w}_2-\tilde{w}_1)]=0, \quad (41)$$

$$D\nabla^8\tilde{w}_i+\frac{Eh}{R_i^2}\frac{\partial^4\tilde{w}_i}{\partial x^4}-\left(1-\eta^2\nabla^2\right)\nabla^4\left\{2\frac{R_i}{R_1}\frac{1}{R_i}N_{x\theta 1}\frac{\partial^2}{\partial x\partial\theta}\right\}\tilde{w}_i$$
$$-\left(1-\eta^2\nabla^2\right)\nabla^4 c\left[\tilde{w}_{i+1}-w_i-(R_{i-1}/R_i)(\tilde{w}_i-\tilde{w}_{i-1})\right]=0;$$
$$i=2,\ldots,k-1, \quad (42)$$

$$D\nabla^8\tilde{w}_k+\frac{Eh}{R_k^2}\frac{\partial^4\tilde{w}_k}{\partial x^4}-\left(1-\eta^2\nabla^2\right)\nabla^4\left\{2\frac{R_k}{R_1}\frac{1}{R_k}N_{x\theta 1}\frac{\partial^2}{\partial x\partial\theta}\right\}\tilde{w}_k$$
$$-\left(1-\eta^2\nabla^2\right)\nabla^4 c\left[(R_{k-1}/R_k)(\tilde{w}_{k-1}-\tilde{w}_k)\right]=0. \quad (43)$$

We consider a set of trial perturbation functions in the sinusoidal harmonic form as follows:

$$\tilde{w}_j(x,\theta)=\tilde{W}_j\sin(m\pi x/L-n\theta),\quad j=1,\ldots,k, \quad (44)$$

where $\tilde{W}_j$ denotes the amplitude of the radial perturbation deflection in j-th layer, with m and n as arbitrary positive integers. Let us define two parameters α and β_i as:

$$\alpha=\frac{m\pi}{L},\quad \beta_i=\frac{n}{R_i}. \quad (45)$$

Insertion of Eq. (44) into Eqs. (41)–(43) gives

$$\tilde{A}_1\sin(\alpha x-n\theta)=0, \quad (46)$$

$$\tilde{A}_i\sin(\alpha x-n\theta)=0;\quad i=2,\ldots,k-1, \quad (47)$$

$$\tilde{A}_k\sin(\alpha x-n\theta)=0, \quad (48)$$

where

$$\tilde{A}_1=D(\alpha^2+\beta_1^2)^4\tilde{W}_1+\frac{Eh}{R_1^2}\alpha^4\tilde{W}_1$$
$$-\left[1+\eta^2(\alpha^2+\beta_1^2)\right](\alpha^2+{\beta_1}^2)^2\left[2N_{x\theta 1}\alpha\beta_1-R_1 p_{\mathrm{vdw},C_{60}}(x){\beta_1}^2\right]\tilde{W}_1$$
$$+R_1{\beta_1}^2\left(\frac{d^4}{dx^4}-\eta^2\frac{d^6}{dx^6}\right)p_{\mathrm{vdw},C_{60}}(x)\tilde{W}_1$$
$$-\left[1+\eta^2(\alpha^2+\beta_1^2)\right](\alpha^2+{\beta_1}^2)^2\left[c(\tilde{W}_2-\tilde{W}_1)\right], \quad (49)$$

$$\tilde{A}_i=D(\alpha^2+\beta_i^2)^4\tilde{W}_i+\frac{Eh}{R_i^2}\alpha^4\tilde{W}_i$$
$$-\left[1+\eta^2(\alpha^2+\beta_i^2)\right](\alpha^2+{\beta_i}^2)^2\left[2\frac{R_i}{R_1}N_{x\theta 1}\alpha\beta_i\right]\tilde{W}_i$$
$$-\left[1+\eta^2(\alpha^2+\beta_i^2)\right](\alpha^2+{\beta_i}^2)^2 c\left[\tilde{W}_{i+1}-\tilde{W}_i-(R_{i-1}/R_i)(\tilde{W}_i-\tilde{W}_{i-1})\right];\ i=2,\ldots,k-1, \quad (50)$$

$$\tilde{A}_k=D(\alpha^2+\beta_k^2)^4\tilde{W}_k+\frac{Eh}{R_k^2}\alpha^4\tilde{W}_k$$
$$-\left[1+\eta^2(\alpha^2+\beta_k^2)\right](\alpha^2+{\beta_k}^2)^2\left[2\frac{R_k}{R_1}N_{x\theta 1}\alpha\beta_k\right]\tilde{W}_k$$
$$-\left[1+\eta^2(\alpha^2+\beta_k^2)\right](\alpha^2+{\beta_k}^2)^2 c\left[(R_{k-1}/R_k)(\tilde{W}_{k-1}-\tilde{W}_k)\right]. \quad (51)$$

For satisfaction of Eqs. (46)–(48) at all x and θ, it is needed that parameters $\tilde{A}_j$ vanish. Accordingly, we have $\overline{A}_j(\alpha,\beta_j)=\int_0^L\tilde{A}_j(\alpha,\beta_j,x)\,dx=0$. Thus, we write

$$\left\{D(\alpha^2+\beta_1^2)^4+\frac{Eh}{R_1^2}\alpha^4-2\left[1+\eta^2(\alpha^2+\beta_1^2)\right](\alpha^2+{\beta_1}^2)^2\alpha\beta_1 N_{x\theta 1}\right.$$
$$+\left[1+\eta^2(\alpha^2+\beta_1^2)\right](\alpha^2+\beta^2)^2\beta^2\left(\frac{R_1}{L}\int_0^L p_{\mathrm{vdw},C_{60}}(x)dx\right)$$
$$\left.+{\beta_1}^2\frac{R_1}{L}\left(\frac{d^3 p_{\mathrm{vdw},C_{60}}(x)}{dx^3}-\eta^2\frac{d^5 p_{\mathrm{vdw},C_{60}}(x)}{dx^5}\right)\right|_0^L\Big\}\tilde{W}_1$$
$$-\left[1+\eta^2(\alpha^2+\beta_1^2)\right](\alpha^2+{\beta_1}^2)^2\left[c(\tilde{W}_2-\tilde{W}_1)\right]=0, \quad (52)$$

$$D(\alpha^2+\beta_i^2)^4\tilde{W}_i+\frac{Eh}{R_i^2}\alpha^4\tilde{W}_i-\left[1+\eta^2(\alpha^2+\beta_i^2)\right](\alpha^2$$
$$+{\beta_i}^2)^2\left[2\frac{R_i}{R_1}N_{x\theta 1}\alpha\beta_i\right]\tilde{W}_i-\left[1+\eta^2(\alpha^2+\beta_i^2)\right](\alpha^2+{\beta_i}^2)^2 c\left[\tilde{W}_{i+1}$$
$$-\tilde{W}_i-(R_{i-1}/R_i)(\tilde{W}_i-\tilde{W}_{i-1})\right]=0;$$
$$i=2,\ldots,k-1, \quad (53)$$

$$D(\alpha^2+\beta_k^2)^4\tilde{W}_k+\frac{Eh}{R_k^2}\alpha^4\tilde{W}_k$$
$$-\left[1+\eta^2(\alpha^2+\beta_k^2)\right](\alpha^2+{\beta_k}^2)^2\left[2\frac{R_k}{R_1}N_{x\theta 1}\alpha\beta_k\right]\tilde{W}_k$$
$$-\left[1+\eta^2(\alpha^2+\beta_k^2)\right](\alpha^2+{\beta_k}^2)^2 c\left[(R_{k-1}/R_k)(\tilde{W}_{k-1}-\tilde{W}_k)\right]=0. \quad (54)$$

Rewriting Eqs. (52)–(54) in the matrix form, we arrive at:

$$[A]_{k\times k}\left\{\tilde{W}\right\}_{k\times 1}-N_{x\theta 1}[B]_{k\times k}\left\{\tilde{W}\right\}_{k\times 1}=0,\quad \text{or } [A-N_{x\theta 1}B]\left\{\tilde{W}\right\}_{k\times 1}=0, \quad (55)$$

where $\left\{\tilde{W}\right\}_{k\times 1}$ is a column matrix composed of components $\tilde{W}_j(j=1,2\ldots,k)$. The nonzero components of the square matrix **A** are given by:

$$A_{11}=D(\alpha^2+\beta_1^2)^4+\frac{Eh}{R_1^2}\alpha^4+\frac{R_1}{L}\beta_1^2\left(\frac{d^3 p_{\mathrm{vdw},C_{60}}(x)}{dx^3}-\eta^2\frac{d^5 p_{\mathrm{vdw},C_{60}}(x)}{dx^5}\right)\Big|_0^L$$
$$+\left[1+\eta^2(\alpha^2+\beta_1^2)\right](\alpha^2+{\beta_1}^2)^2\left[c+\frac{R_1}{L}\beta_1^2\int_0^L p_{\mathrm{vdw},C_{60}}(x)dx\right],$$
$$A_{(i)(i-1)}=-c\left[1+\eta^2(\alpha^2+\beta_i^2)\right](\alpha^2+{\beta_i}^2)^2(R_{i-1}/R_i);\quad i=2,\ldots,k-1,$$
$$A_{(i)(i)}=D(\alpha^2+\beta_i^2)^4+\frac{Eh}{R_i^2}\alpha^4$$
$$+c\left[1+\eta^2(\alpha^2+\beta_i^2)\right](\alpha^2+{\beta_i}^2)^2\left[1+(R_{i-1}/R_i)\right];\quad i=2,\ldots,k-1,$$
$$A_{(i)(i+1)}=-c\left[1+\eta^2(\alpha^2+\beta_i^2)\right](\alpha^2+{\beta_i}^2)^2;\quad i=2,\ldots,k-1,$$
$$A_{(k)(k)}=D(\alpha^2+\beta_k^2)^4+\frac{Eh}{R_k^2}\alpha^4+c\left[1+\eta^2(\alpha^2+\beta_k^2)\right](\alpha^2+{\beta_k}^2)^2(R_{k-1}/R_k). \quad (56)$$

Also, the components of the diagonal matrix $\boldsymbol{B}$ are given by:

$$B_{(j)(j)} = 2\frac{R_j}{R_1}\left[1+\eta^2(\alpha^2+\beta_j^2)\right](\alpha^2+{\beta_j}^2)^2\alpha\beta_j. \quad (57)$$

Now, we seek the non-trivial solution $\left\{\tilde{W}\right\}_{k\times 1}$ for Eq. (55). For existence of such a solution, the determinant of $[\boldsymbol{A}-N_{x\theta\ 1}\boldsymbol{B}]$ must be set to zero:

$$\det[A-N_{x\theta 1}B]=0. \quad (58)$$

Now, we look for the eigenvalues $N_{x\theta 1}$ appeared in Eq. (58). For a considered m and n, we may have k possibly different solutions for $N_{x\theta 1}$. It is noted that any value for $N_{x\theta 1}$ is related to a specific torsional moment through Eq. (34). Denoting the minimum positive value of eigenvalues $N_{x\theta 1}$ for a considered m and n as $(N_{x\theta 1})_{m,n}$, the corresponding critical torsional moment of (m,n) mode of perturbation is obtained as:

$$T_{m,n} = 2\pi(N_{x\theta 1})_{m,n}\left(\sum_{j=1}^{k} R_j^3\right)/R_1. \quad (59)$$

The critical torsional moment T_{cr} of the MWCNP is the minimum value of $T_{m,n}$ for different m and n. In the special case of C_{60}@SWCNT peapod, we obtain

$$T_{m,n} = \pi R^2 \frac{1}{\alpha\beta_1(\alpha^2+\beta_1^2)^2\left[1+\eta^2(\alpha^2+\beta_1^2)\right]}\times \left(D(\alpha^2+\beta_1^2)^4+\frac{Eh}{R_1^2}\alpha^4+\frac{R_1}{L}{\beta_1}^2\left(\frac{d^3p_{vdw,C_{60}}(x)}{dx^3}-\eta^2\frac{d^5p_{vdw,C_{60}}(x)}{dx^5}\right)\right|_0^L + \left[1+\eta^2(\alpha^2+\beta_1^2)\right](\alpha^2+{\beta_1}^2)^2\left[\frac{R_1}{L}\beta_1^2\int_0^L p_{\mathrm{vdw},C_{60}}(x)dx\right]\Bigg). \quad (60)$$

5. Numerical results

The C_{60}@(10,10) CNP is a specific C_{60}-peapod with an interest between researchers to investigate its properties [10,12,14–16]. In this section, we present some numerical results for this specific nano-peapod. The values used for parameters in the numerical analyses have been extracted from [24] in which $D=0.85$ eV, $Eh=360$ J m^{-2}, $h=0.34$ nm, and $R=0.678$ nm have been reported. The C_{60} fullerenes, in the case of high density packing, portray a linear one-dimensional crystal into (10,10) CNT with lattice equilibrium distance $D_f=1$ nm [9,12,41]. The vdW internal pressure distribution exerted by C_{60} encapsulated fullerenes on (10,10) CNT is considered in accordance with what reported in Ref. [18]. The results obtained in this section are based on one term approximation of Eq. (5).

Now, consider a single unfilled (10,10) CNT with length $L=12.62$ nm, noting that the length has been extracted from Shibutani and Ogata [42]. The obtained critical torsional moment T_{cr} of the (10,10) CNT versus η is shown in Fig. 2 for the common range of $\eta<1$ nm [27,29,31].

It is obvious that the nonlocal formulation of this paper results in a lower T_{cr} than that is given by the classical theory, noting that the nonlocal formulation reduces to the classical formulation if we set $\eta=0$. This lesser prediction reduces the difference of the classical theory based result, i.e., the value 5.04 nN.nm which corresponds to $\eta=0$ nm, from that of the MD simulation, i.e., the value of 1 nN nm [42]. It is noted that from the MD simulation we have the value of $\tau_{x\theta}=N_{x\theta 1}/h\approx 1$ *GPa* for the considered nanotube on the onset of the torsional instability reported by Shibutani and Ogata [42] which results in the mentioned MD-based value of 1 nN nm for $T_{cr}=2\pi R^2 h\ \tau_{x\theta}$. According to the Figure, with a value 0.7 nm for η, the nonlocal formulation gives the buckling torque in an appropriate agreement with the MD simulation.

Here, the CNT with $L=12.62$ nm is considered to be filled with a high density packing of C_{60}, i.e., $D_f\approx 1$ nm [9,12,41]. The results for the critical torsional moment T_{cr} of the considered C_{60}@(10,10) CNP together with the corresponding results of the single unfilled (10,10) CNT have been shown at different vales of η in Fig. 3.

The results show that the existence of C_{60} fullerenes in the CNT causes an increase in the critical torsional moment T_{cr}. It indicates the more resistance of the C_{60}@(10,10) CNP against the instability comparing it with the (10,10) CNT. This is a common agreement between researchers. Due to the encapsulation of C_{60} fullerenes, the resistance against the buckling instability of (10,10) CNT under axial compressive load [12,13] and bending moment [14] has been reported to be enhanced. Specially, the increase in the torsional instability resistance for the (10,10) CNT with encapsulated C_{60} fullerenes have been predicted previously based on the MD simulations [15,16].

In Fig. 4, the percentage of increase in T_{cr} for C_{60}@(10,10) CNP with respect to the corresponding (10,10) CNT has been depicted versus η for some different lengths L.

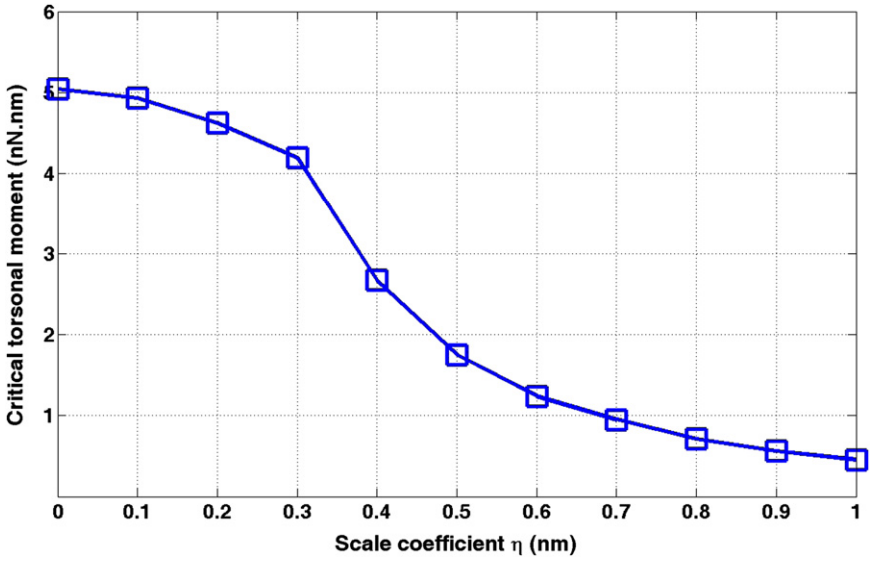

Fig. 2. Critical torsional moment of the (10,10) CNT with $L=12.62$ nm versus scale coefficient η.

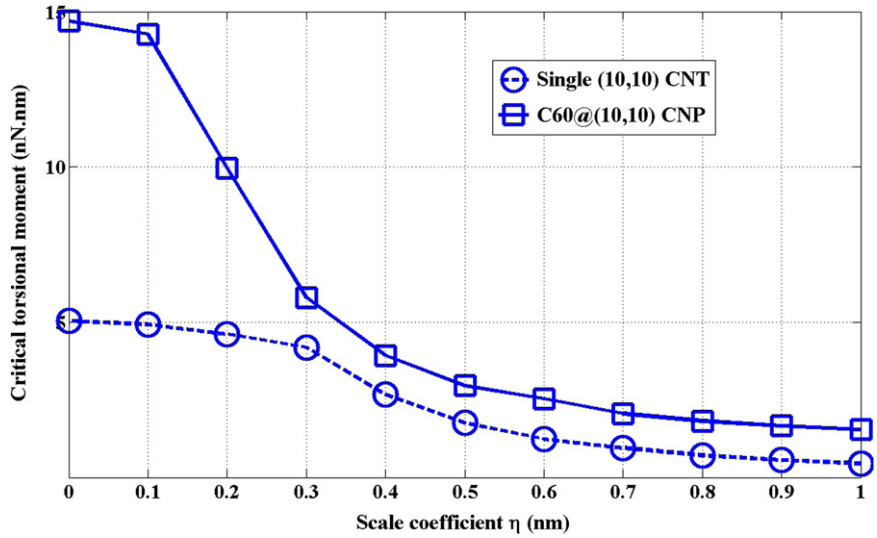

Fig. 3. Critical torsional moment T_{cr} of the C_{60}@(10,10) CNP and single (10,10) CNT with $L=12.62$ nm versus the scale coefficient η.

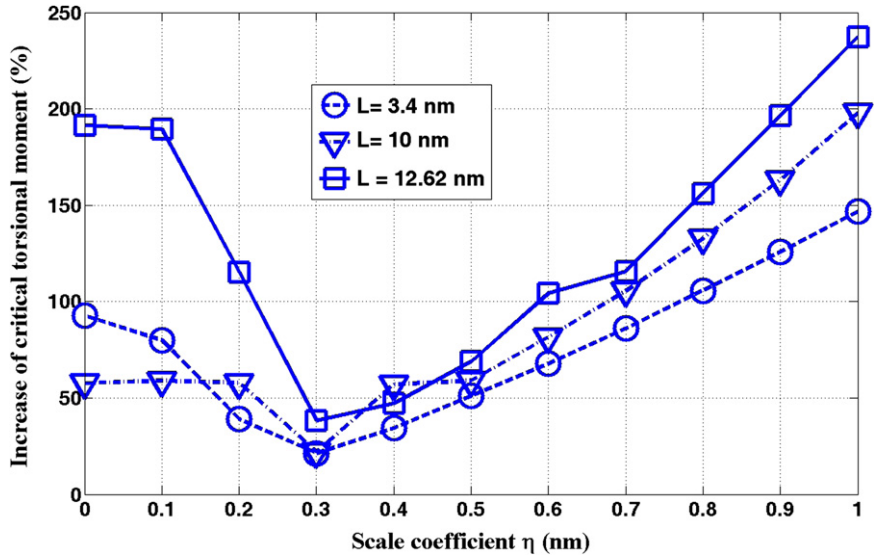

Fig. 4. The percentage of increase in T_{cr} for C_{60}@(10,10) CNP with respect to the corresponding (10,10) CNT.

Based on MD simulations, Jeong et al. [15] reported a value of 111.2% increase in the torsional critical moment of a (10,10) CNT with length of $L=10$ nm due to enclosing a high density packing of C_{60} fullerenes. In another MD work, Wang [16] reported a value of 140% increase in the torsional buckling resistance of a (10,10) CNT with length $L=3.4$ nm by filling it with high density packing of C_{60} fullerenes. From Fig.4, it is observed that the amount of increase percentage in the critical torsional moment similar to the amount reported by Wang [16] for $L=3.4$ nm can be obtained based on the formulation of this work if the scale coefficient is chosen approximately as $\eta=0.9$ nm. Also, the amount of increase percentage similar to what reported by Jeong et al. [15] for $L=10$ nm is predicted by the nonlocal formulation of this work with about $\eta=0.7$ nm; recalling that with this value for η, the prediction of the nonlocal formulation for the critical torsional moment of a single nanotube will also be in good agreement with the MD simulations [42].

According to the nonlocal shell formulation of this work, the scale coefficient $\eta=e_0a$ is evaluated between 0.7 and 0.9 nm for appropriate agreement with available MD simulations [15,16,42]. It is noted that in the literature, the range of $\eta<2$ nm has been estimated for SWCNT [19,27]. The evaluated value for η in this work between 0.7 and 0.9 nm is within this range.

6. Conclusions

Due to the expensive computational cost of atomistic simulations of nanostructers, some researchers are interested in continuum based approaches. However, the classical continuum theory is not able to appropriately analyze the nanostructures which have crucial discontinuities between their atoms. The nonclassical theories, with specific parameters provided in their formulations in order to capture the small-scale effects, posses the benefits of the continuum based approaches without expensive computational costs. The nonlocal theory is one of the nonclassical theories which has widely been implemented recently by researchers for simulation of nanostructures. In this paper, a formulation has been derived for studying the torsional stability of CNPs using the nonlocal Donnell shell model. The obtained numerical results from the presented formulation for the buckling torsional moment computed in case studies for

single (10,10) CNT and also the percentage of its increase for the C_{60}@(10,10) CNP are relatively in a good agreement with some MD results available in the literature. It is observed that the encapsulated C_{60} fullerenes inside the (10,10) CNT cause an increase in the resistance against the torsional instability more than 100%. It is concluded that utilizing the nonlocal continuum theory can significantly diminish the gap between the classical continuum theory predictions and results of MD simulations in the case of torsional instability of CNTs and CNPs.

References

[1] M.W. Cole, V.H. Crespi, G. Stan, C. Ebner, J.M. Hartman, S. Moroni, M. Boninsegni, Physical Review Letters 84 (2000) 3883.
[2] M.S. Dresselhaus, K.A. Williams, P.C. Eklund, MRS Bulletin 24 (1999) 45.
[3] H. Gao, Y. Kong, Annual Review of Materials Research 34 (2004) 123.
[4] A. Kuznetsova, D.B. Mawhinney, V. Naumenko, J.T. Yates Jr, J. Liu, R.E. Smalley, Chemical Physics Letters 321 (2000) 292.
[5] X. Zhao, Y. Ando, Y. Liu, M. Jinno, T. Suzuki, Physical Review Letters 90 (2003) 187401.
[6] B.W. Smith, M. Monthioux, D.E. Luzzi, Nature 396 (1998) 323.
[7] M. Monthioux, Carbon 40 (2002) 1809.
[8] B.W. Smith, M. Monthioux, D.E. Luzzi, Chemical Physics Letters 315 (1999) 31.
[9] B. Burteaux, A. Claye, B.W. Smith, M. Monthioux, D.E. Luzzi, J.E. Fischer, Chemical Physics Letters 310 (1999) 21.
[10] S. Osaka, S. Saito, A. Oshiyama, Physical Review Letters 86 (2001) 3835.
[11] D. Qian, W.K. Liu, R.S. Ruoff, Physical Review Letters 105 (2001) 10753.
[12] B. Ni, S. Sinnott, P. Mikulski, J. Harrisson, Physical Review Letters 88 (2002) 205505.
[13] L. Zhou, B.E. Zhu, Z.Y. Pan, Y.X. Wang, J. Zhu, Nanotechnology 18 (2007) 275709.
[14] J. Zhu, Z.Y. Pan, Y.X. Wang, L. Zhou, Q. Jiang, Nanotechnology 18 (2007) 275702.
[15] B.-W. Jeong, J.-K. Lim, S.B. Sinnott, Journal of Applied Physics 101 (2007) 084309.
[16] Q. Wang, Carbon 47 (2009) 507.
[17] A.N. Sohi, R. Naghdabadi, Acta Materialia 55 (2007) 5483.
[18] A.N. Sohi, R. Naghdabadi, Carbon 45 (2007) 952.
[19] Y.Y. Zhang, C.M. Wang, W.H. Duan, Y. Xiang, Z. Zong, Nanotechnology 20 (2009) 395707.
[20] X.Q. He, S. Kitipornchai, K.M. Liew, Journal of the Mechanics and Physics of Solids 53 (2005) 303.
[21] C.Q. Ru, Journal of Applied Physics. 89 (2000) 3425.
[22] C.Q. Ru, Physical Review B 62 (2000) 10405.
[23] H.K. Yang, X. Wang, Simulation in Materials Science and Engineering 14 (2006) 99.
[24] X. Wang, H.K. Yang, K. Dong, Materials Science and Engineering: A 404 (2005) 314.
[25] J. Peddieson, G.R. Buchanan, R.P. McNitt, International Journal of Engineering Science 41 (2003) 305.
[26] J.N. Reddy, International Journal of Engineering Science 45 (2007) 288.
[27] Y.-G. Hu, K.M. Liew, Q. Wang, X.Q. He, B.I. Yakobson, Journal of the Mechanics and Physics of Solids 56 (2008) 3475.
[28] N. Challamel, C.M. Wang, Nanotechnology 19 (2008) 345703.
[29] Q. Wang, C.M. Wang, Nanotechnology 18 (2007) 075702.
[30] C.M. Wang, Y.Y. Zhang, X.Q. He, Nanotechnology 17 (2006) 1.
[31] R. Li, G.A. Kardomateas, ASME Journal of Applied Mechanics 74 (2007) 399.
[32] A.C. Eringen, International Journal of Engineering Science 10 (1972) 1.
[33] A.C. Eringen, Journal of Applied Physics 54 (1983) 4703.
[34] K.T. Chan, Y.P. Zhao, The dispersion characteristics of the waves propagating in a spinning single-walled carbon nanotube, Science China: Physics, Mechanics and Astronomy 54 (2011) 1854.
[35] M. Asghari, R. Naghdabadi, J. Rafati-Heravi, Physica E 43 (2011) 1050.
[36] Y.Q. Zhang, G.R. Liu, X. Han, Physical Review B 70 (2004) 1.
[37] M.J. Hao, X.M. Guo, Q. Wang, European Journal of Mechanics—A/Solids 29 (2009) 49.
[38] R. Li, G.A. Kardomateas, Journal of Applied Mechanics -T. ASME 74 (2007) 1087.
[39] Yin Gen-Wei Wang, Ya-Pu Zhang, Zhao, Gui-Tong Yang, Journal of Micromechanics and Microengineering 14 (2011) 1119.
[40] L.H. Donnell, Beams Plates, and Shells, McGraw-Hill, New York, 1976.
[41] M. Melle-Franco, H. Kuzmany, F. Zerbetto, The Journal of Physical Chemistry B 107 (2003) 6986.
[42] Y. Shibutani, S. Ogata, Simulation in Materials Science and Engineering 12 (2004) 599.